DOI: 10.1002/anie.201204331

High Oxidation States

Spectroscopic Observation of a Group 12 Oxyfluoride: A Matrix-Isolation and Quantum-Chemical Investigation of Mercury Oxyfluorides**

Lester Andrews, Xuefeng Wang, Yu Gong, Tobias Schlöder, Sebastian Riedel, and Marvin J. Franger*

Mercury has a diverse and interesting chemistry in both solution and solid state.[1] Yellow solid HgO precipitates on the addition of OH^- to mercuric cation solutions, and the direct combination of Hg and O_2 in air for long periods at elevated temperatures gives red solid HgO, which reverts to the elements on heating to 400 °C, and thus provides a laboratory source for oxygen gas.[2] The stable form of mercuric oxide contains -O-Hg-O-Hg- chains with linear O-Hg-O subunits.[3] All four HgX_2 dihalides are solid compounds,[1] and molecular HgF_2 and $HgCl_2$ have been observed in matrix isolation experiments.[4–7]

In the last two centuries, mercury has been employed as a common laboratory fluid for temperature and pressure measuring devices (thermometers, manometers, McLeod gauges, etc.), but the toxicity of mercury has limited these earlier applications in today's work places. As a result, mercury has been avoided more and more, and mercury thermometers have been largely replaced by alcohol thermometers. However, amalgams have been used as dental fillings since the mid-1800s.[8–10] The ease of preparation of filling material by mixing liquid mercury and a metal alloy such as Permite (84% Ag and Sn as major components) is noteworthy.[11]

[*] Prof. L. Andrews, Prof. X. Wang, Dr. Y. Gong
Department of Chemistry, University of Virginia
Charlottesville, VA 22904-4319 (USA)
Prof. X. Wang
Department of Chemistry, Tongji University
Shanghai, 200092 (P.R. China)
Dipl.-Chem. T. Schlöder, Dr. S. Riedel
Albert-Ludwigs Universität Freiburg
Institut für Anorganische und Analytische Chemie
Albertstrasse 21, 79104 Freiburg (Germany)
E-mail: sriedel@psichem.de
M. J. Franger
Guest collaborator, Dentist
2250 Old Ivy Road, Charlottesville, VA 22903 (USA)

[**] L.A. gratefully acknowledges financial support from DOE Grant DE-SC0001034 and NCSA computing Grant CHE07-0004N. S.R. thanks the DFG project HA 5639/3-1 and the Fonds der Chemischen Industrie (FCI) for financial support, the BWGrid cluster for computational resources, and Profs. I. Krossing and H. Hillebrecht for their generous and continuous support.

Supporting information for this article (computed data, anion structure, and computational details) is available on the WWW under http://dx.doi.org/10.1002/anie.201204331.

The laser ablation technique has been used by Andrews and co-workers to sublimate atoms for reaction partners since the late 1980s.[12–15] Red phosphorus was laser ablated to generate phosphorus atoms; solid boron worked better as a laser target, because boron is much harder than red phosphorus.[13] Subsequently, harder more refractive metals, such as Ta, Re, Os, W, Th, and U, have been laser ablated to provide reactive atoms.[14,15] During the pulsed laser ablation process (laser focused to less than 0.1 mm diameter spot), surface temperatures reach more than 3000 K,[16] and metal atoms evaporate translationally and electronically excited, often in metastable states, which survive transit to the cold surface (4–7 K) for condensation and reaction with gases (such as O_2, CO, H_2, CH_4, CH_3F, and CCl_4 diluted in matrix host gases Ar, N_2, Ne, and H_2).[14,15,17] This work is an evolution of the matrix isolation technique developed by Pimentel and co-workers beginning in the 1950s.[18]

Herein we use OF_2 as an efficient reaction partner with mercury atoms as a test case and to prepare new mercury oxyfluorides. Mercury chemistry remains an active research field,[19–23] and laser-ablated mercury atom reactions with other small molecules will follow from these laboratories.

Mercury is the lowest-melting metal (m.p. −39 °C), and is a liquid at room temperature,[1] and thus Hg does not remain in place to be ablated by a focused, pulsed laser beam. In early matrix-isolation investigations, Hg atoms were evaporated slightly above room temperature (the vapor pressure of Hg is about 1 millitorr at 20 °C),[24] and intense electronic absorption spectra were observed in a series of matrix hosts.[25] Reactions of Hg with H_2, H_2O, or F_2 have been investigated by exciting the Hg atoms with a mercury arc discharge lamp (such as the common street lamp, 175 W, which costs about US$ 10).[7,26–29]

Thus, evaporation and excitation of Hg atoms by laser ablation requires Hg in some solid form. Pressed discs of HgO and $HgCl_2$ were used in one of these laboratories without success. Thus, it occurred to one of the corresponding authors, during an appointment at the dentist, to use a common dental filling as a laser ablation target and thus a source of Hg atoms. The dentist and coauthor M. Franger prepared two Hg-Permite alloy[11] solids shaped as lumps (5 mm diameter, 3 mm thick), which were used for the first experiments reported herein (analysis 800 mg of Permite and 696 mg of Hg: 46.5% by weight Hg). Mercury was added to the first filling material to give 49.0% Hg by weight and pressed into a mold (ca. 6.4 mm diameter hole drilled through a ca. 3.2 mm stainless steel plate with a removable back plate) as a proof of

principle. Another target contained 67% Hg and 33% permite, which was used as a dental filling in the early 20th century.[8]

Laser-ablation matrix-isolation experiments were thus performed with mercury atoms following the methods described previously.[13,14,17,30] IR spectra from the reactions of laser-ablated mercury-amalgam target material, 46.5% Hg (Amal), with 1% $^{16}OF_2$ in excess argon are compared in Figure 1 with spectra using a specially prepared 67% Hg (Amal) target. Absorptions from reaction products previously identified include the OF radical, $^{116,118,120}SnO_2$, $^{63,65}CuF_2$, HgF_2, $^{107,109}AgF_2$, SnF_2, and AgF, and a new product from the silver reaction with OF_2.[4,5,31–34] A new weak absorption at 472.2 cm^{-1} is appropriate for HgF based on the gas phase fundamental of 482.7 cm^{-1}.[35] Experiments were also performed with Hg(Na) (Aldrich), and the 90% Hg (10% Na) reaction product spectra are also compared in Figure 1. The NaF absorption is observed at 495 cm^{-1}.[26] Product bands from new mercury bearing species are marked OHgF and FOHgF and listed in Table 1. The observation of HgF_2 and HgF bands indicates reaction and suggests that the formation of new HgO_xF_y species is expected. Corresponding experiments were done with $^{18}OF_2$ in excess argon, and isotopic shifts were observed for several new product bands.

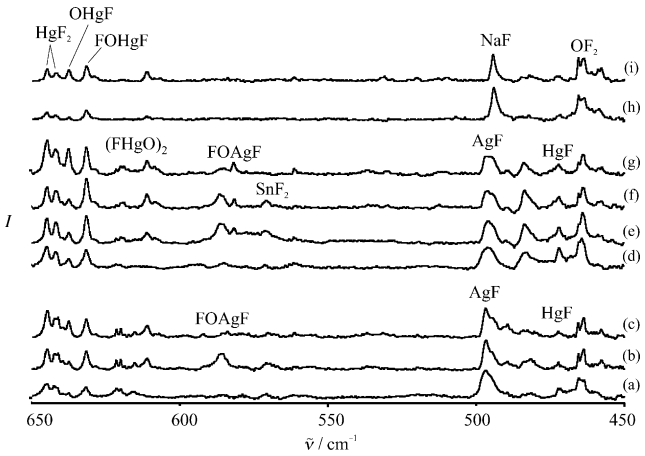

Figure 1. IR spectra following co-deposition of laser-ablated Hg atoms from solid amalgams with OF_2 (1%) in excess argon for 60 min. a) Hg 46.5%, permite; b) after annealing to 20 K; c) after full arc (>220 nm) irradiation; d) Hg 67%, permite; e) after annealing to 20 K; f) after annealing to 30 K; g) after full arc irradiation; h) Hg 90%, Na, after annealing to 20 K; i) after full arc (>220 nm) irradiation.

Table 1: Computed and experimental frequencies [cm^{-1}] and intensities [km mol^{-1}] using CCSD(T) and B3LYP methods.[a]

OHgF							
CCSD(T)		B3LYP		Expt Ne		Expt Ar	
^{16}O	^{18}O	^{16}O	^{18}O	^{16}O	^{18}O	^{16}O	^{18}O
648.3	636.1	631.9 (77)	619.1 (85)	648.0	635.9	637.6	625.2
568.9	548.6	554.5 (12)	535.7 (4)				
182.8	178.0	181.6 (12)	176.9 (12)				
175.7	170.1	172.4 (14)	167.9 (14)				
FOHgF							
^{16}O	^{18}O	^{16}O	^{18}O	^{16}O	^{18}O	^{16}O	^{18}O
865.1	837.6	938.4 (24)	909.4 (24)				
641.2	632.9	619.7 (96)	611.2 (98)	640.5	632.5	631.6	623.4
566.0	543.7	548.7 (4)	527.1 (0.1)				
247.9	245.3	253.0 (6)	250.0 (5)				
174.1	170.0	168.0 (11)	164.1 (10)				
120.8	121.0	118.8 (8)	118.7 (8)				

[a] Asymmetric stretching vibration for HgF_2: 655.5 (CCSD(T)), 636.0 (B3LYP), 657.5 (neon), 645 (argon).[7]

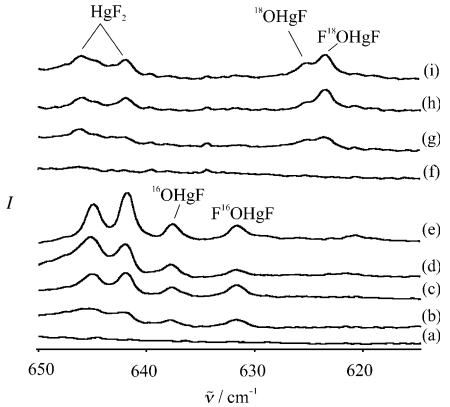

Figure 2. IR spectra following co-deposition of Hg atoms (vapor pressure at 45°C) with OF_2 (1%) in excess argon for 60 min. a) $^{16}OF_2$, b) full arc (>220 nm) irradiation for 10 min; c) after annealing to 20 K; d) full arc irradiation for 15 further minutes; e) after annealing to 30 K; f) $^{18}OF_2$. g)–i) follow the same treatment as (b)–(d).

Figure 2 compares IR spectra of the two most important new absorptions using both $^{16}OF_2$ and $^{18}OF_2$ precursors. These spectra were recorded following thermal Hg vapor deposition with the precursor in excess argon and Hg arc irradiation. The two new absorptions at 637.6 and 631.6 cm^{-1} just below HgF_2 show oxygen isotopic shifts of 12.4 and 8.2 cm^{-1}, respectively. Similar experiments were performed in excess neon, and anticipated blue-shifts were observed in the product absorptions: the OF radical shifted to 1031.1 cm^{-1} and HgF_2 to 652.6 cm^{-1}. The new absorptions of interest were observed in neon at 648.0 and 640.5 cm^{-1}, with isotopic counterparts given in Table 1.

The new absorption at 631.6 cm^{-1} is stronger and it shows less variation on annealing and sample irradiation than the 637.6 cm^{-1} band mentioned above. The stronger band increases on annealing to 20 and 30 K, whereas the weaker 637.6 cm^{-1} band decreases. However, full arc irradiation increases the 637.6 cm^{-1} band while the 631.6 cm^{-1} absorption decreases slightly. The anticipated FOHgF insertion product is predicted to have its strongest mode, the Hg–F absorption, just below that for OHgF, but different mode mixing results in 8.3 (CCSD(T)) or 8.5 cm^{-1} (B3LYP) oxygen isotopic shifts for FOHgF (Table 1).

Several minimum energy structures for mercury oxyfluoride species have been located by structure optimizations at the coupled-cluster and DFT levels (Figure 3). Note that OHgF gives a linear structure at the CCSD(T)/aug-cc-pVTZ level with a O–Hg bond distance of 194.9 pm, whereas the

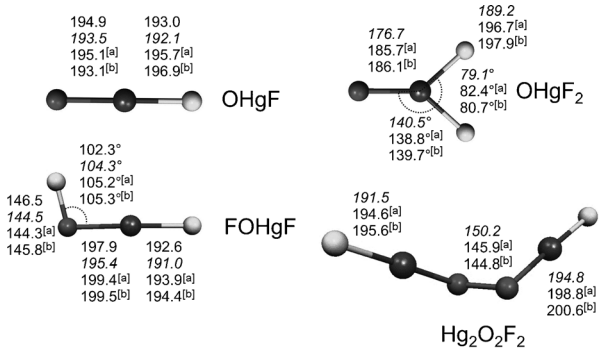

Figure 3. Optimized structures of mercury oxyfluoride molecules. Normal text: CCSD(T); *italics*: SCS-MP2; [a] B3LYP, [b] BP86. Angles of $Hg_2O_2F_2$: Hg-O-O *102.5*, 106.9,[a] 109.0[b]; Hg-O-O-Hg *−160.1*, −130.5,[a] −111.2.[a]

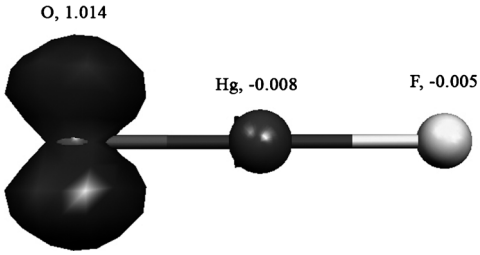

Figure 4. Mulliken atomic spin densities at the B3LYP level; isosurface plot: ±0.001 a.u.

Hg–F length is computed to be 193.0 pm. The reaction energy calculated for $OHgF \rightarrow Hg + OF$ shows an endothermic decomposition channel of 178 kJ mol^{-1} at the CCSD(T)/aug-cc-pVTZ level, thus emphasizing its stability, which is in accord with its experimental preparation under cryogenic conditions in rare-gas matrixes.

Vibrational frequencies for this simple OHgF oxyfluoride were computed at the DFT and CCSD(T) levels, and the strongest new absorption is predicted just below HgF_2 with a ^{16}O to ^{18}O shift of 12.2 or 12.8 cm^{-1} (Table 1), which is in excellent agreement with the 637.6 cm^{-1} band and its ^{18}O counterpart at 625.2 cm^{-1}. This is the antisymmetric O-Hg-F stretching mode, and the shift for ^{18}O-Hg-F is correspondingly smaller than the hypothetical linear O-Hg-O diradical would have. The strong Hg–F stretching mode for the FOHgF insertion product is predicted at the CCSD(T) level to be 7.1 cm^{-1} below the value for OHgF and to be a less-coupled Hg–O, Hg–F stretching mode with only 8.3 cm^{-1} of ^{18}O shift, which is again in excellent agreement with our observed values.

At first, it seems likely that OHgF could be described as an open-shell Hg^{III} metal center forming an Hg=O double bond and an Hg–F single bond. However, as shown by previous quantum-chemical calculations, the formal +III oxidation state of mercury is unlikely to exist even in HgF_3.[19,36] A closer inspection of the OHgF molecule indeed confirms the assumption that mercury is not oxidized beyond the oxidation state +II. At first, the Hg–O bond length is even longer than the Hg–F bond, and description as a Hg=O double bond is therefore unlikely. Beyond the bond length comparison, we have computed the spin density distribution of the OHgF molecule (Figure 4). The isosurface plot of the spin density clearly shows that the spin density is mainly located at the oxygen center and not at the mercury atom. The latter behavior would be expected if the mercury center were oxidized beyond the oxidation state +II. We therefore assign the mercury center to the formal oxidation state +II and the new oxyfluoride can be described as an ·OHgF radical. The further dimerization reaction of two ·OHgF radicals has been computed as well (Table 1), and the weaker band at 611.2 cm^{-1} is probably due to this dimer species.

The dimerization of OHgF is computed to be exothermic by −168 kJ mol^{-1} at the B3LYP/def2-TZVPP level, and the peroxide structure in Figure 1 is the most-stable configuration. The doubly bridged oxygen structure containing a formally Hg^{III} atom is 352 kJ mol^{-1} higher in energy using B3LYP/def2-TZVPP. The peroxide bond formed shows a distance of 145.9 pm at B3LYP level (150.2 pm at SCS-MP2), which is in agreement with the experimental value of H_2O_2 of 147.5 pm[37] and the peroxide bond in $[(\eta^2\text{-}O_2)IrO_2]$ of 145.1 pm.[38] Beyond these OHgF monomer and dimer compounds, we also investigated other possible mercury oxyfluoride species, such as Hg bond insertion into OF_2, forming the FOHgF molecule (Figure 1). This compound shows only C_s symmetry owing to the F-O-Hg angle of 102.3° at CCSD(T)/aug-cc-pVTZ level (Figure 1).

This molecule is also calculated to be thermochemically stable. Its decomposition reaction $FOHgF \rightarrow Hg + OF_2$ is computed to be 211 kJ mol^{-1} at the CCSD(T)/aug-cc-pVTZ level, which is even more stable than the open-shell molecule ·OHgF (see the Supporting Information, Table SI1). Formally, this species contains mercury in oxidation state +II, whereas its isomer $OHgF_2$ (Figure 3) would correspond to an formal oxidation state of +IV, as known for $Hg^{IV}F_4$.[7] Nevertheless, singlet $OHg^{IV}F_2$ is computed to be much higher in energy, by 231 kJ mol^{-1}, than its $FOHg^{II}F$ isomer. Furthermore, its decomposition channel into Hg and OF_2 is calculated to be exothermic by −109 kJ mol^{-1} at the SCS-MP2/def2-TZVPP level, which has been shown to perform reliably for HgF_4.[39] It is therefore highly unlikely for this species to be formed under cryogenic conditions in rare-gas matrixes. Coupled-cluster calculations of $OHgF_2$ show very high T_1 diagnostic values of 0.068, which most likely indicate a multi-reference character of the wavefunction.

It is well-known that laser ablation provides a source of electrons together with hard UV light.[40] These circumstances can lead to the formation of anions, which are captured in the matrix under cryogenic conditions, such as the recently characterized trifluoride monoanion $[F_3]^-$.[41] Therefore, we have also investigated the $[OHgF]^-$ anion (Supporting Information, Figure SI1). This closed-shell species shows a linear structure in which the Hg–O bond (190.1 pm) is shorter than the Hg–F bond (203.1 pm) at the CCSD(T)/aug-cc-pVTZ level (Supporting Information, Figure SI1). Its reaction energy is computed to be endothermic by 249 kJ mol^{-1} at the CCSD(T)/aug-cc-pVTZ level. Unfortunately, this anion is not detected here because of the relatively low yield of the OHgF radical. We have also investigated the

structures and stabilities of binary mercury fluoride anions, such as $[HgF_5]^-$ and $[HgF_6]^{2-}$, as shown in the Supporting Information, Figure SI1.

In conclusion, excited Hg atoms react with OF_2 to form the first Group 12 oxyfluoride, OHgF, with Hg in the +II oxidation state, and the insertion product FOHgF. Mercury amalgams serve as effective laser ablation target sources of Hg atoms for reactions and provide complementary photochemistry to that for the products of UV irradiated samples prepared from thermally evaporated mercury atoms. The stabilization of Group 12 metals in their formal oxidation state of +III remains still a challenge.

Methods

Calculations were performed at various levels of density functional theory (DFT) and at ab initio levels SCS-MP2 and CCSD(T). DFT and SCS-MP2 calculations were carried out with the Turbomole V6.3[42] program package and the analytical gradient methods implemented therein. The gradient-corrected BP86[43,44] functional and the hybrid functional B3LYP[45–47] as implemented in Turbomole were used. The selection of B3LYP was based on its excellent performance for the redox thermochemistry of transition-metal systems in high oxidation states.[48] GGA functionals (BP86) tend to overestimate the stability of the higher oxidation states,[39] as do Møller–Plesset perturbation (MP2) calculations. However, it was found that the SCS-MP2 method provides very reliable thermochemical data for Hg^{IV} species.[39] Coupled-cluster calculations with single and double substitutions (CCSD), as well as with inclusion of perturbative triple excitations (CCSD(T) level) were carried out with the MOLPRO 2006 program package.[49] All of the species have been fully optimized at a given computational level. For more computational details, see the Supporting Information.

Received: June 4, 2012
Published online: July 18, 2012

Keywords: fluorine · high oxidation states · matrix isolation · mercury · oxyfluorides

[1] F. A. Cotton, G. Wilkinson, C. A. Murillo, M. Bockman, *Advanced Inorganic Chemsitry, Vol. 6*, Wiley, New York, **1999**.
[2] N. N. Greenwood, A. Earnshaw, *Chemistry of the Elements*, Pergamon, Oxford, **1984**.
[3] S. Biering, A. Hermann, J. Furthmuller, P. Schwerdtfeger, *J. Phys. Chem. A* **2009**, *113*, 12427.
[4] A. Loewenschuss, A. Ron, O. Schnepp, *J. Chem. Phys.* **1969**, *50*, 2502.
[5] A. Givan, A. Loewenschuss, *J. Chem. Phys.* **1976**, *65*, 1851.
[6] D. E. Tevault, D. P. Strommen, K. Nakamoto, *J. Am. Chem. Soc.* **1977**, *99*, 2997.
[7] X. Wang, L. Andrews, S. Riedel, M. Kaupp, *Angew. Chem.* **2007**, *119*, 8523; *Angew. Chem. Int. Ed.* **2007**, *46*, 8371.
[8] E. W. Skinner, *The Science of Dental Materials, 6 ed.*, Saunders, Philadelphia, **1967**.
[9] J. L. Ferracane, *Materials in Dentistry: Principles and Applications*, Lippincott, Williams & Wilkins, Philadelphia, **2001**.
[10] J. A. Soncini, N. N. Maserejian, *J. Am. Dent. Assoc. JADA J. Am. Dent. Assoc.* **2007**, *138*, 763.
[11] Dent. Assoc. Materials Data Sheet: ermite dental alloy composition: 56% Ag, 28% Sn, 15% Cu, 0.5% In, and 0.2% Zn by weight.
[12] L. Andrews, R. Withnall, *J. Am. Chem. Soc.* **1988**, *110*, 5605.
[13] T. R. Burkholder, L. Andrews, *J. Chem. Phys.* **1991**, *95*, 8697.
[14] L. Andrews, H.-G. Cho, *Organometallics* **2006**, *25*, 4040.
[15] R. D. Hunt, L. Andrews, *J. Chem. Phys.* **1993**, *98*, 3690.
[16] D. B. Geohegan in *Laser Ablation: Mechanisms and Applications-II*, *AIP Conference Proceedings 288* (Ed.: J. C. Miller), American Institute of Physics, Knoxville, **1993**.
[17] L. Andrews, *Chem. Soc. Rev.* **2004**, *33*, 123.
[18] E. Whittle, D. A. Dows, G. C. Pimentel, *J. Chem. Phys.* **1954**, *22*, 1943.
[19] S. Riedel, M. Kaupp, P. Pyykkö, *Inorg. Chem.* **2008**, *47*, 3379.
[20] P. Zaleski-Ejgierd, P. Pyykkö, *J. Phys. Chem. A* **2009**, *113*, 12380.
[21] J. Kim, H. Ihee, Y. S. Lee, *J. Chem. Phys.* **2010**, *133*, 144309.
[22] P. Zaleski-Ejgierd, P. Pyykkö, *Phys. Chem. Chem. Phys.* **2011**, *13*, 16510.
[23] S. Knecht, S. Fux, R. van Meer, L. Visscher, M. Reiher, T. Saue, *Theor. Chem. Acc.* **2011**, *129*, 631.
[24] M. L. Huber, A. Laesecke, D. G. Friend, NISTR 6643, Boulder, CO, **2006**.
[25] L. Brewer, B. Meyer, G. D. Brabson, *J. Chem. Phys.* **1965**, *43*, 3973.
[26] N. Legay-Sommaire, F. Legay, *J. Phys. Chem.* **1995**, *99*, 16945.
[27] X. Wang, L. Andrews, *Inorg. Chem.* **2004**, *43*, 7146.
[28] X. Wang, L. Andrews, *Inorg. Chem.* **2005**, *44*, 108.
[29] V. A. Macrae, T. M. Greene, A. J. Downs, *Phys. Chem. Chem. Phys.* **2004**, *6*, 4586.
[30] M. Zhou, L. Andrews, C. W. Bauschlicher Jr., *Chem. Rev.* **2001**, *101*, 1931.
[31] L. Andrews, J. I. Raymond, *J. Chem. Phys.* **1971**, *55*, 3078.
[32] J. W. Hastie, R. H. Hauge, J. L. Margrave, *J. Mol. Spectrosc.* **1973**, *45*, 420.
[33] A. Bos, J. S. Ogden, *J. Phys. Chem.* **1973**, *77*, 1513.
[34] Unpublished results.
[35] K. P. Huber, G. Herzberg, *Molecular Spectra and Molecular Structure*, *4*: *Constants of Diatomic Molecules*, Van Nostrand Reinhold, New York, **1979**.
[36] P. Hrobárik, M. Kaupp, S. Riedel, *Angew. Chem.* **2008**, *120*, 8759; *Angew. Chem. Int. Ed.* **2008**, *47*, 8631.
[37] A. F. Holleman, E. Wiberg, *Lehrbuch der Anorganischen Chemie*, *Vol. 102*, Walter de Gruyter, Berlin, **2007**.
[38] Y. Gong, M. Zhou, M. Kaupp, S. Riedel, *Angew. Chem.* **2009**, *121*, 8019; *Angew. Chem. Int. Ed.* **2009**, *48*, 7879.
[39] S. Riedel, M. Kaupp, *Coord. Chem. Rev.* **2009**, *253*, 606.
[40] R. Flesch, M. C. Schurmann, M. Hunnekuhl, H. Meiss, J. Plenge, E. Ruhl, *Rev. Sci. Instrum.* **2000**, *71*, 1319.
[41] S. Riedel, T. Köchner, X. Wang, L. Andrews, *Inorg. Chem.* **2010**, *49*, 7156.
[42] TURBOMOLE V 6.2.
[43] J. P. Perdew, *Phys. Rev. B* **1986**, *33*, 8822.
[44] A. D. Becke, *Phys. Rev. A* **1988**, *38*, 3098.
[45] A. D. Becke, *J. Chem. Phys.* **1993**, *98*, 5648.
[46] C. Lee, W. Yang, R. G. Parr, *Phys. Rev. B* **1988**, *37*, 785.
[47] B. Miehlich, A. Savin, H. Stoll, H. Preuss, *Chem. Phys. Lett.* **1989**, *157*, 200.
[48] S. Riedel, M. Straka, M. Kaupp, *Phys. Chem. Chem. Phys.* **2004**, *6*, 1122.
[49] MOLPRO 2006.1 a package of ab initio programs.

